University of Nebraska - Lincoln

DigitalCommons@University of Nebraska - Lincoln

12-2021

A Method for Visualizing Water Flow through Modified Root Zones

Dallas M. Williams
University of Nebraska - Lincoln

Follow this and additional works at: https://digitalcommons.unl.edu/agronhortdiss

Part of the Agricultural Science Commons, Agriculture Commons, Agronomy and Crop Sciences Commons, Botany Commons, Horticulture Commons, Other Plant Sciences Commons, and the Plant Biology Commons

A METHOD FOR VISUALIZING

WATER FLOW THROUGH MODIFIED ROOT ZONES

by

Dallas M. Williams

A THESIS

Presented to the Faculty of

The Graduate College at The University of Nebraska

In Partial Fulfillment of Requirements

For the Degree of Master of Science

Major: Agronomy

Under the Supervision of Professor Roch Gaussoin

Lincoln, Nebraska

December, 2021

A METHOD FOR VISUALIZING
WATER FLOW THROUGH MODIFIED ROOT ZONES

Dallas M. Williams, M.S.

University of Nebraska, 2021

Advisor: Roch Gaussoin

As the number of impervious surfaces in urban environments increases, the ability of modified root zones to infiltrate water is becoming more important. Current methods of tracing water flow through soil profiles include excavating large pits in situ or analyzing soil cores in the laboratory with computed tomography or magnetic resonance imaging. While useful, these methods may not be suitable for urban settings or practical in every laboratory. We propose a new method that is less invasive, does not require extensive technical equipment and can reliably trace water movement through the soil profile in order to calculate flow rate based on the advancement of the wetting front. It was also realized that recording soil resistance during sampling could provide a better understanding of soil conditions influencing water movement. In this study soil cores 30 cm in length and 7.62 cm in diameter were obtained from golf course putting greens and green fluorescent water tracing dye was used in conjunction with UV light and time lapse photography to track movement of the wetting front. Images were processed with MATLAB and an algorithm was developed to quantify flow rates in mm sec^{-1}. A soil sampler with a load cell sensor recorded the soil resistance during sampling. The flow patterns captured in this study illustrate the quick initial movement of water through

preferential pathways and the slower absorption of micropores as infiltration progresses. This method has the potential to provide quality information on flow path development and evolution, changes in soil layering over time and flow rates during water infiltration.

ACKNOWLEDGEMENTS

Acknowledgements are needed as this thesis was the result of the collaborative efforts and diligent work from several individuals. First, I want to thank my advisor Dr. Roch Gaussoin for accepting me as his last graduate student, I will be forever grateful for the opportunity. Thank you to my undergraduate mentor and committee member Dr. Humberto Blanco for all of his guidance and support in my career in soil science. Thank you to Dr. Keenan Amundsen for serving on my committee and all of your advice.

A special thank you is required for those who helped in the development of this project. To Hessan Sedaghat, undergraduate student of the PIE group in Biological Systems Engineering Department at University of Nebraska, Lincoln, for construction and programming of the soil sampler, thank you! To Dr. Yufeng Ge of the Biological Systems Engineering Department at the University of Nebraska, Lincoln for developing the algorithm and your assistance with image processing, thank you! To Kelsey Karnik, doctoral student in the Statistics Department, for your expertise and guidance in statistical analysis of the datasets, thank you! To our research technicians, Matt Sousek and Craig Ferguson for building various prototypes, thank you! This research could not have been accomplished without each of your time and dedication.

I want to give my utmost appreciation to my parents for all of their support and encouragement during my education, I could not have gotten this far without you. And, lastly, thank you to my best friend and my other half- the other Dallas. You'll never know how much you mean to me and how much I appreciate you for just being there when I needed you.

TABLE OF CONTENTS

LIST OF TABLES

LIST OF FIGURES

INTRODUCTION

Soil has been called the first filter of Earths water (Clothier et al. 2008). Soil filters water via infiltration, or the downward entry of water into the soil (Hillel, 2004). There has been significant research on water infiltration into agricultural soils (Feuki et al. 2012, Babaei et al. 2018, Skaalsveen et al 2019) because of intense soil management, high input of agro-chemicals and the importance of global food supply (Keestra et al. 2016). However, as urban development and the amount of impervious surfaces continues to increase, proper water management in cities is becoming more important (Hamilton and Waddington 1999, Woltemade 2010, Armson et al. 2013, Ren et al. 2020). Urban soils are distinct from agricultural soils in that they often contain modified root zones either intentionally or because of topsoil removal during construction (Hamilton and Waddington 1999, Bigelow and Soldat 2013).

Modified root zones are often constructed to minimize compaction risks and optimize water movement while supporting plant growth (Fisher, 2017). Modified root zones are typically used where highly trafficked native soils must support cultural activities and adequate plant growth. Popular examples of systems that rely on modified root zones include golf course putting greens, rain gardens, roof gardens and green roofs, street tree pits, and sports fields. The design of the root zone will depend on the expected levels of use (frequency and intensity), maintenance resources and management needs (DePew and Guise 2001). However, the designs considered most effective use tailored sand, silt, and clay particle sizes to ensure optimal water drainage and capillary retention important for plant growth (Wightman 1994).

Modified root zones that are sand based are known to withstand high intensity use and a wide range of weather conditions, making them ideal for sports fields and golf course putting greens (DePew and Guise 2001). The macropores created by sand particles result in high drainage and aeration capabilities but low water and nutrient holding capacities (Bigelow et al. 2001). Therefore, it is common for modified root zones to employ a hanging water column to increase water retention (Bigelow et al. 2001, Prettyman and McCoy 2003, McCarty et al. 2016). A hanging water column is created by textural discontinuities resulting from the presence of a fine-textured sand above a coarse gravel layer (Fisher 2017).

Even when proper soil specifications are used to ensure high drainage and aeration, water infiltration into modified root zones can be affected by many factors. As turfgrass root zones age, organic matter accumulates, and water infiltration decreases (Lewis et al. 2010). The opposite has been found in home lawns, largely as a result of poorer soil physical properties post construction (Hamilton and Waddington 1999, Woltemade 2010). Infiltration and percolation can also be hindered by the formation of distinct soil layers, water repellant soils that are hydrophobic in nature and excessive thatch-mat accumulation.

Over time, from natural settling and infiltrating water, fine soil particles like silt and clay can move deeper into the soil profile, deceasing macroporosity and creating distinct layers (Anderson et al. 2008, Lewis et al. 2010, McCarty et al. 2016). A decrease in root zone oxygen can lead to anaerobic conditions resulting in a hydrogen sulfide rich, toxic black layer (Woodham 2013, Berndt 2016). Iron layers form when iron oxidizes

where a saturated sand layer overlies a drier gravel layer often resulting in a cemented layer (Obear et al. 2014). The formation of these soil layers creates a barrier which impedes water movement.

Water repellant soils, or hydrophobic soils, are characterized by the presence of organic, waxy materials that coat soil particles and resist surface infiltration until much of the soil becomes wetted (Bauters et al. 1998, Dekker et al. 2001, Nektarios et al. 2007). Water repellency is especially common in sandy soils because of its low surface areas, as well as turfgrass systems because of high organic matter production (McCarty et al. 2016). Water repellant soils can induce unstable wetting fronts leading to losses via preferential flow (Hendrickz et al. 1993, Bauters et al. 1998, Carrillo et al. 2000, Ritsema et al. 2004, Nimmo 2012). Preferential flow refers to the rapid transport of water and solutes through a small portion of the soil profile typically via cracks in soil structure, worm holes, root channels and/or large macropores (Merdun et al. 2008, Allaire et al. 2009).

When organic matter accumulates on the surface of turfgrass soils it is referred to as thatch. It is widely known that as thatch accumulates air-filled porosity and infiltration rates decrease (Gaussoin et al. 2007). Excess thatch seals the soil surface leading to turf stress and possible black layer formation (Cockerham et al. 2012). The afore mentioned factors that inhibit percolation can easily lead to anaerobic soil conditions that deprive plant roots of oxygen and give rise to poor turf growth, health, and development (DePew and Guise 2001, Fisher 2017).

McCarty et al. (2016) has stated the key to success for commercial turfgrass facilities is proper water management. There are numerous economic and environmental implications linked to a soils ability to infiltrate and percolate water (ASTM 2003, Bevard 2009, Filipovic et al. 2015, McCarty et al. 2016, Hopmans et al. 2017). Water infiltration and the subsequent transfer of water in soils, known as percolation, can be considered the interaction between matrix flow and preferential flow (Jarvis 2007, Legout et al. 2009, Zhang et al. 2016). Soil matrix flow describes water movement through the bulk soil body and is important for plant growth because it becomes plant available water (Zhang et al. 2017). Flow through preferential pathways is the quick vertical movement of water that has been shown to increase the risk of solute transport and groundwater contamination (Hendrickz et al. 1993, Flury et al. 1994, Ritsema et al. 2001) and create spatial variability of soil water affecting plant growth (Bauters et al. 1998, Schneider et al. 2018).

Dyes have long been used to stain and analyze flow paths and soil structure (Flury et al. 1994, Noguchi et al. 1999, Anderson et al. 2008, Kodesova et al. 2011, Schneider et al. 2018). By excavating the soil to examine flow paths, dye tracing provides greater insight into the multi-dimensional flow domain (Wang et al. 2006). After excavation, photographs are typically taken of the dye paths and analyzed with image analysis software (Hendrickz et al. 1993, Bauters et al 1998). The main disadvantage to dye tracing in situ is that excavating the soil is labor intensive and highly disruptive, therefore repeated measurements are limited and difficult to obtain at the same site (Flury et al. 1994, Anderson et al. 2008, Mossadeghi-Bjorklund et al. 2018).

Dye tracing can also be done in the laboratory with packed or undisturbed soil cores (Kohne and Mohanty 2005). In the lab, the wetting front can be tracked with time lapse photography or video recordings of flow paths into cores with transparent casings (Hill and Parlange 1972, Bauters et al. 1998, Allaire et al. 2009) or with more technical instruments like magnetic resonance imaging and x-ray computed tomography (Luo and Lin 2009, Kodesova et al. 2011, Sammartino et al. 2012). While computed tomography and other high-resolution scanners enable reconstruction and visualization of soil structure in an intact soil core (Kaestner et al. 2008, Luo et al. 2008), these machines can be quite expensive and may not be practical in every laboratory.

To date, the information gained from dye tracing has been limited to qualitative analysis, and some quantitative analysis, of soil structure, flow paths and/or pore characteristics (Allaire et al. 2009). Percolation or flow rate has been confined to solute transport and break through curves (Zhou and Selim 2001, Tonguc and Merdun 2009, Stumpp et al. 2012, Hassan et al. 2010, Hassanpour et al. 2019) and outflow rates (Kohne and Mohanty 2005, Filipovic et al. 2015). No other study has attempted to directly quantify rate of water flow through the soil profile. However, such information would be useful in understanding how water moves through the profile and soil layers. More specifically, deeper knowledge about how management techniques can affect water movement and soil layer formation could be gained.

We propose an improved laboratory method for tracing water movement through modified rootzones that is reliable, efficient, less invasive and does not require extensive technical equipment. Soil cores 30 cm x 7.62 cm were used in combination with a

fluorescent dye tracer and UV light to study water infiltration. Soil core length matches the depth of the primary root zone in a two tier putting green (USGA, 2018). Water movement was captured using time lapse photography and images analyzed with MATLAB software to derive percolation rate based on advancement of the wetting front highlighted by the fluorescent water tracing dye.

Measurement of water movement through different soil layers by quantifying percolation rate in mm sec^{-1} rather than cm hr^{-1} (Johnson 1963, ASTM 2003) will increase precision. We hope to better predict water movement in modified rootzones. The goal of this study was to develop a new method to quantify water percolation rates in mm sec^{-1} to distinguish different soil layers of a modified rootzone. The objectives of this research was to 1) develop a method to visualize the flow of water through modified root zones without extensive technical equipment, 2) develop an algorithm to accurately and reliably follow the movement of the wetting front and 3) based on the advancement of the wetting front, calculate percolation rate in mm sec $^{-1}$. During the project a fourth objective was added to 4) simultaneously measure soil resistance when obtaining column samples.

MATERIALS AND METHODS

Experimental Location

Soil cores were obtained from the practice putting greens of two City of Lincoln public golf courses, Mahoney Golf Course (Mahoney) and Holmes Park Golf Course (Holmes), and one experimental putting green on the East Campus of the University of Nebraska (East Campus) in Lincoln, NE. All putting greens sampled were constructed with an intermediate layer, however, they differed in green age, root zone composition, and management styles (Table 1). The putting green on East Campus is an experimental plot and the specific management practices change depending on the research conducted. The managers at East Campus maintain the plots at putting green quality. Soil samples were collected at all locations in Fall 2020.

Table 1. Construction year, root zone composition at time of construction, and management practices during the sampling year, 2020, for two public golf courses (Holmes and Mahoney) and one University of Nebraska research putting green (East Campus) in Lincoln, NE.

Location	Year Constructed	Root Zone Composition	Aeration	Topdressing	Fertilizer
Holmes	1960	Native soil with unknown percent of sand incorporated on-site	Spring- solid tine Fall- cored 1.27 cm width Backfilled with #10 sand	Weekly- verticut and topdressed with G sand	N- 15 gm^{-2} P & K- 7.5 gm^{-2}
Mahoney	1976	USGA specifications	Spring- solid tine Fall- cored 1.27 cm width Backfilled with #10 sand	Weekly- verticut and topdressed with G sand	N- 15 gm^{-2} P & K- 7.5 gm^{-2}
East Campus	2016	85/15 #10 sand and Dakota peat moss	Monthly- solid tine 0.64 cm width Spring & Fall- verticut two directions to 0.48 cm depth	Biweekly- light application of G sand	N- 10 gm^{-2}

Soil Probe Apparatus

Multiple attempts were made to build a soil sampler that was as simple as possible to meet our original objectives. Initially, samples were taken by pounding a mylar cylinder protected in PVC casing with a sledgehammer. This method proved very difficult to reach the desired 30 cm depth, especially when the root zone was very dry. The sledgehammer method was quickly abandoned, and a soil probe was fashioned out of a standard cup cutter. Also, a stainless steel cylinder was built to replace the PVC casing (Figure 1). The steel cylinder was more durable and better protected the soil core from disturbance compared to the PVC casing. There were two holes near the top of the steel cylinder where a hook could be placed to remove the cylinder from the putting green.

The cup cutter soil probe was able to reach the desired 30 cm depth and was used to take many samples. However, the quality of the soil cores varied depending on the person taking the sample. It was realized that people with longer and/or stronger arms needed fewer strikes with the cup cutter in order to drive the cylinder 30 cm which, in turn, produced lower variability among similar samples. This did not meet our criteria of a method that is reliable and efficient. Therefore, a soil probe was built using a truck jack and was powered with a handheld, cordless power drill (Figure 2).
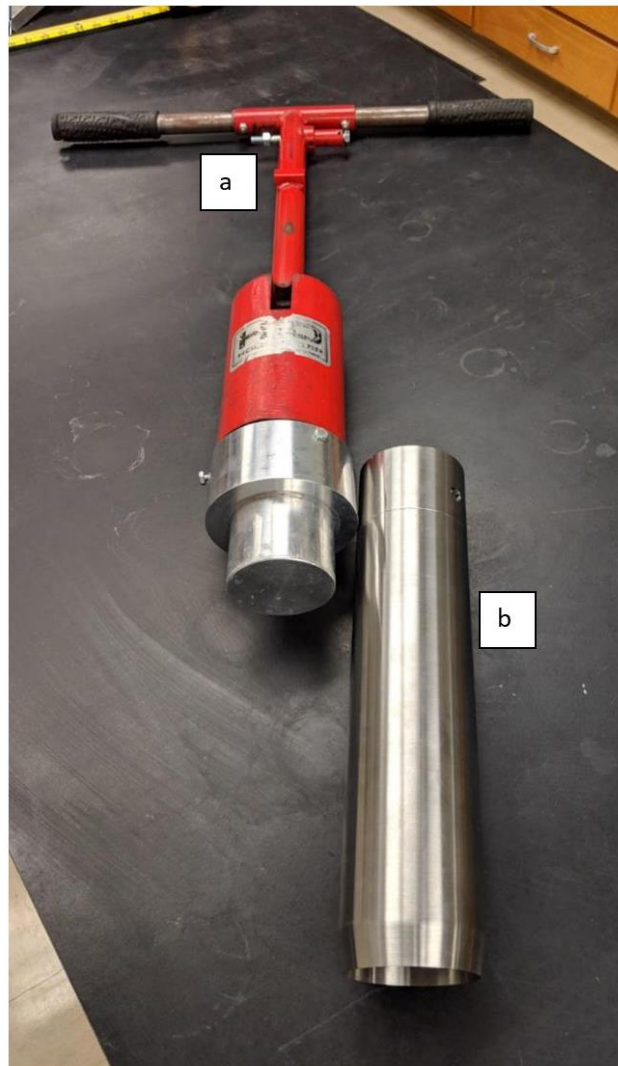
Figure 1. The first soil probe built to remove 30 cm soil cores from golf course putting greens was constructed from a cup cutter (a). Also pictured is the stainless steel sleeve fabricated to house the transparent, mylar cylinder during soil sampling (b).

Figure 2. The second soil probe built to take 30 cm soil cores from golf course putting greens. This soil probe used a hydraulic truck jack (a) to push the soil core into the ground. Also pictured is the stainless steel sleeve (b) in position for collecting a sample, the four augers (c) needed to keep the soil probe in place during sampling, and the anchor spots where augers are inserted with a hand-held drill (d).

The truck jack was turned upside down to drive the soil core into the root zone. The truck jack powered soil probe was anchored to the ground with four augers that were inserted into place with the handheld drill. This probe worked very well and produced consistent soil cores, regardless of who was taking the sample. After approximately 40 samples were taken with this probe, the jack broke, and it could no longer be used. Another soil probe was built using a heavy-duty jack that could withstand more vigorous use. This probe was used with great success, but there were still ways to optimize the soil probe. One area for improvement was the actuation method, which could be made more consistent with a motor. Further, it was realized that if the force being applied to the soil core during sampling could be recorded, this information could be used to further examine soil profile layering and its effect on water movement.

An automated soil probe was built by the Programming Instrumentation and Electronics (PIE) group within the Biological Systems Engineering (Programming Instrumentation and Electronics (PIE) | College of Engineering (unl.edu)) department at the University of Nebraska, Lincoln (Figure 3). The probe is approximately 1.3 m tall and .5 m wide. It is equipped with a custom built controller box that features both touch screen display and physical switches to operate the soil probe and monitor the data during sampling (Figure 4). Just below the controller box is the main unit which houses the connectors for the controller box, batteries and motor driver (NovalithIC BTS 7960, Infineon Technologies, Neubiberg, Germany). On either side of the main unit there is a 12V battery. This probe is mounted on wheels for easy transport and requires augers to anchor the probe while taking a soil sample. The soil sampler was programmed by the

PIE group of the Biological Systems Engineering Department at UNL and was based on

an Arduino microcontroller.

A significant improvement of this soil probe was the FA-HD-2200-24-H-15 linear

actuator (Firgelli, Ferndale, WA) and a LC202-5K load cell sensor (Omega, Norwalk,

CT). The linear actuator used a hall effect encoder to control speed and direction, as well

as record its position within the profile. The max load of the actuator was 2,200 lbs. The

load cell sensor was mounted to the tip of the actuator and recorded the applied force in

compression (pushing the soil core into the ground) and tension (removing the soil

sample from the ground). The steel cylinder that holds the mylar cylinder sits just below

the load cell sensor. The data recorded from the load cell sensor during sampling was

plotted in real-time and saved to an SD card for later analysis. An amplifier (HX711,

Avia Semiconductor, Xiamen, P.R. China) was used to read the data from the load cell.
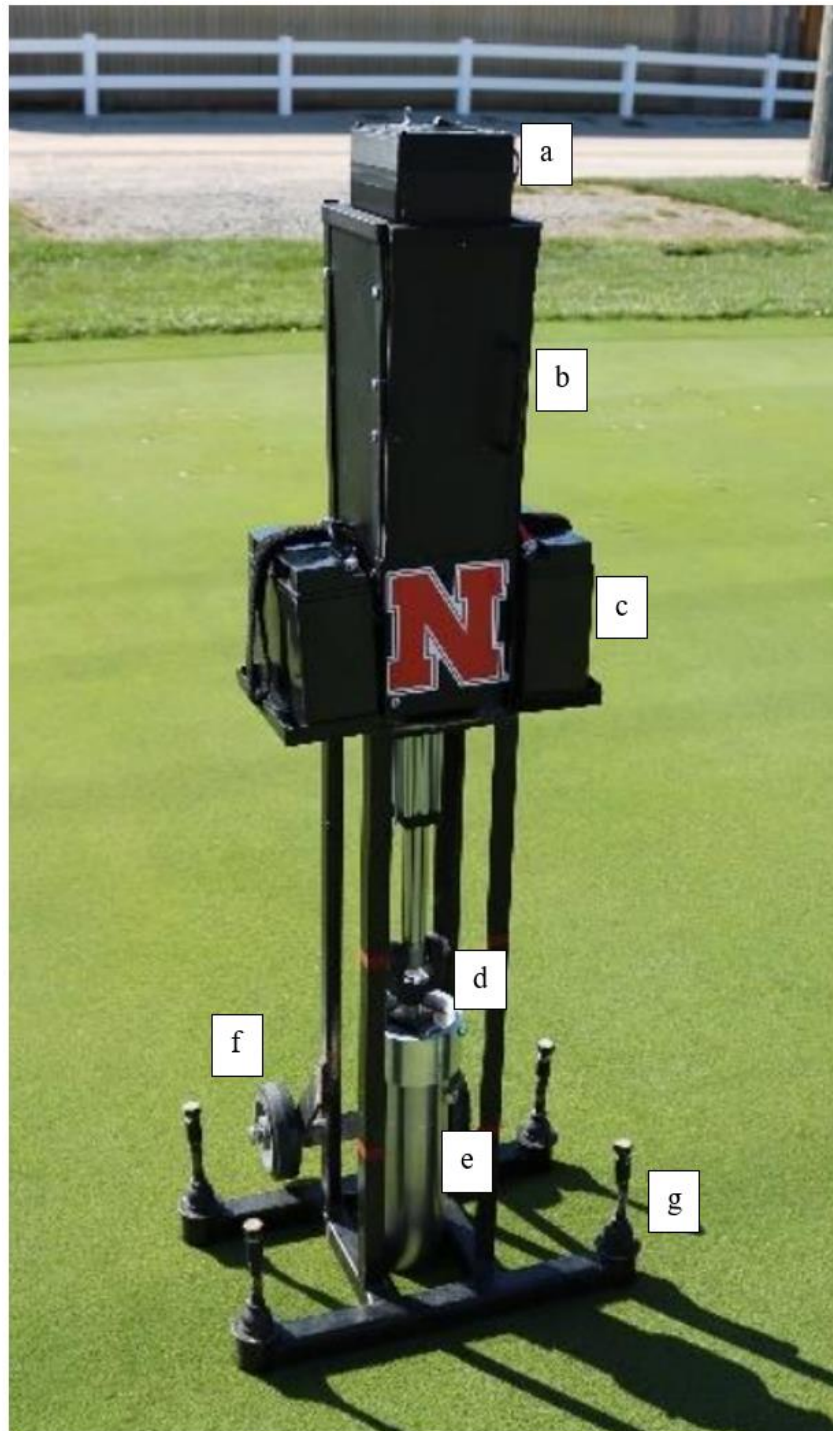
Figure 3. The final soil probe built by the Programming, Instrumentation and Electronics group of the Biological Systems Engineering Department of UNL that features a) the controller box, b) main unit, c) battery located either side of main unit, d) linear actuator and load cell sensor, e) steel sleeve with soil sample, f) wheels for easy transport, and g) anchor spots with augers in place.
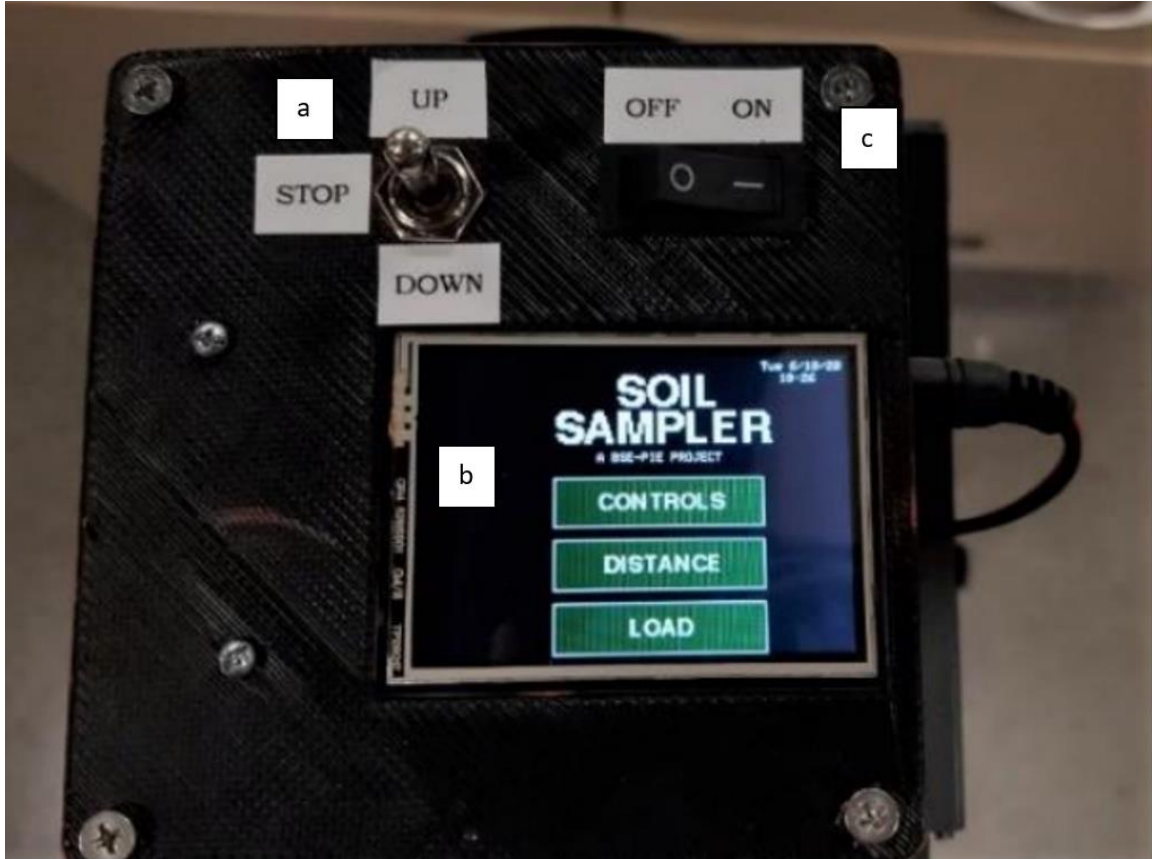
Figure 4. The controller box component of the soil sampler that is used to power on the machine (c) and take a soil sample to 30 cm depth using either a) physical switches or the b) touch screen display. The touch screen can also be used to monitor soil resistance data during sampling.

Soil Sample Collection

Soil samples were collected in transparent, mylar cylinders 30 cm in length and 7.62 cm in diameter. Prior to sampling, the insides of the mylar cylinders were treated with a hydrophobic ceramic coating called Nano Bond (Nano Bond, USA). Each cylinder received two coats of the polymer. Two coats are better than one to ensure complete coverage and there was no difference between two and three coats. The hydrophobic

coating was used to resist water from adhering to the cylinder walls and promote uniform infiltration.

Before sampling, the soil probe must be anchored down to withstand high resistance profile layers. A handheld drill is used to insert and remove the augers into anchor spots on the sampler. Cylinders were put inside the stainless steel sleeve in order to eliminate damage during sampling (Figure 5). The automated soil probe was used to take five samples per putting green (Figure 6) to a depth of 30 cm. Cores were taken to a depth of 30 cm because this is the depth of a USGA putting green at construction. The disturbance to the putting green was minimal. The area where the core was removed was backfilled with sand and the holes left by augers were easily repaired, similar to ball mark repair (Figure 7). Soil cores were capped on both ends to minimize disturbance during transportation to the laboratory and subsequent storage. Soil cores were stored at 4° C until analysis. Soil cores should not be stored below 0° C, as freezing and thawing highly disrupts soil structure and produces flow pattern not indicative of the original root zone.

Figure 5. A stainless steel sleeve was fabricated to protect the transparent mylar cylinders from buckling during soil sampling on golf course putting greens.

Figure 6. Soil cores 30 cm in length taken from the practice putting green at Mahoney golf course in Lincoln, Nebraska. Soil cores were taken in transparent cylinders in order to capture flow patterns with time lapse photography during the dye tracing experiment.

Figure 7. There is minimal disturbance to the putting green after the soil sample has been removed and the hole backfilled with sand (a). The holes left by the augers can be easily fixed similar to a ball mark repair (b).

Tension Table Apparatus

Golf course putting greens employ a hanging water column to create uniform water content and retain moisture and nutrients (Bigelow et al. 2001, USGA 2002, McCoy and McCoy 2009). A hanging water column forms when a fine textured soil overlies a coarse textured soil and creates an interface that prevents the movement of water until much of the overlying soil has been wetted (Bigelow et al. 2001, McCarty et al. 2016). Consequently, at the interface, a small negative tension exists (Bigelow et al. 2001). As such, the hanging water column technique was used in the laboratory to mimic

this tension. A tension table, able to hold only one soil core at a time, was constructed per

Dane and Hopmans (2002) to apply suction to the bottom of the core (Figure 8). Tension

should be set at -3.33 cm, which is the negative tension being applied to a putting green

root zone at the perched water table interface (30 cm) as measured by Waltz Jr. et al.

(2003).
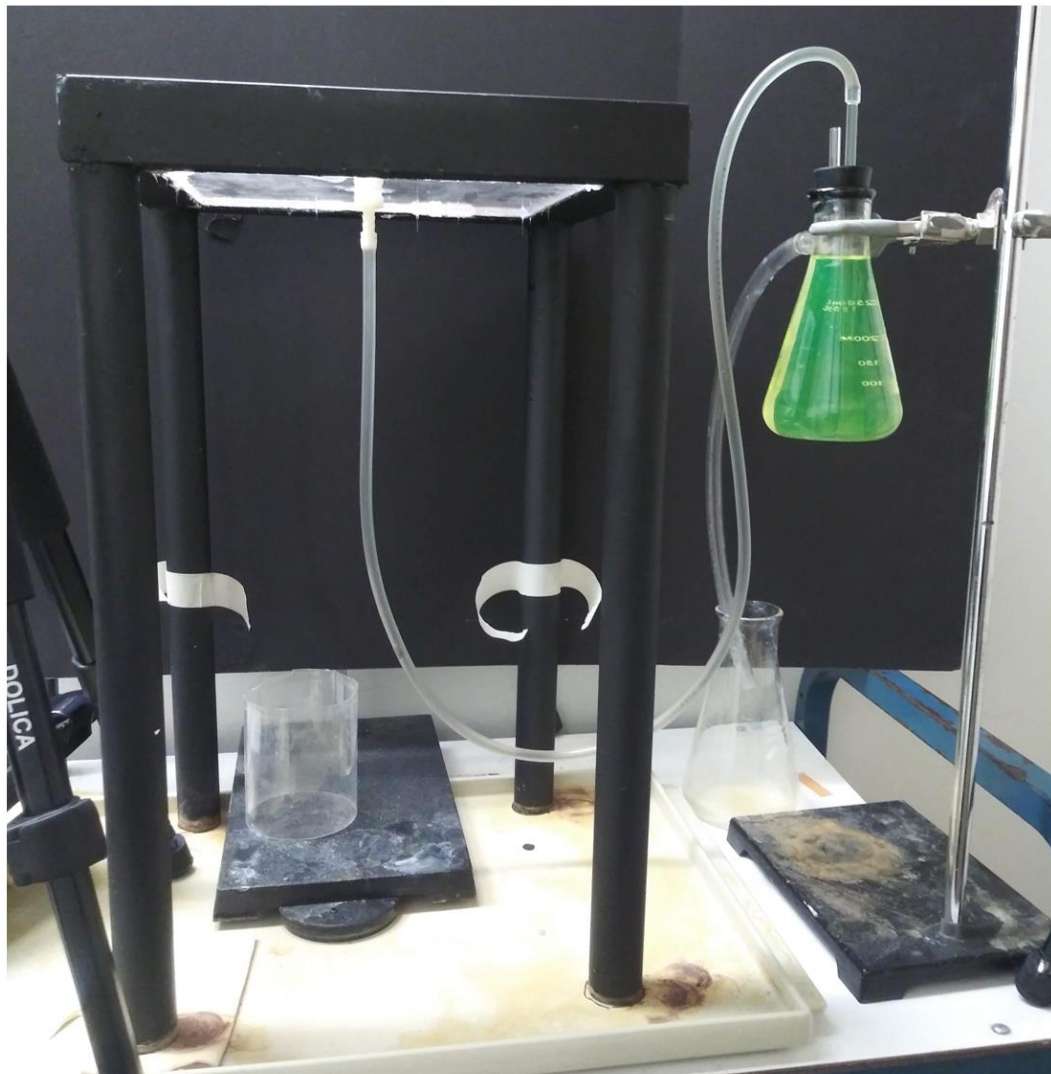
Figure 8. A tension table was constructed to replicate the hanging water column effect that occurs at the sand-gravel interface 30 cm below the surface of golf course putting greens. The tension table applied -3.33 cm tension to the bottom of the soil core during dye tracing.

Dye Tracing

Soil samples were analyzed in a dark room at the University of Nebraska, Lincoln (UNL). The dark room is a small room with no windows. Inside this room is a tension table with time lapse photography cameras on either side, facing each other, in order to capture water movement on both sides of the soil core (Figure 9). A large UV light was situated above the table and cameras to minimize shadowing as much as possible. A mylar cylinder with a black cap that had a single hole drilled into the center was used to apply dye onto the soil surface. A ring stand with an adjustable clamp was used to hold the dye delivering cylinder above the soil core (Figure 10).

To visualize water flow through the transparent soil core, a UV fluorescent water tracing dye (Factory Direct Chemicals, USA) was used. The dye is commonly used in plumbing for leak detection, flow mapping, rate and volume analysis, and retention time studies, among other applications. The dye is diluted with water to a 1:10 ratio. A green dye was used for tracing water movement.

Water movement was captured using time lapse photography. Two cameras were used to capture flow on the left and right side of the core. This was done to strengthen data analysis and in case one side of the core resisted wetting and could not be used for image analysis. Cameras should be placed as close to the tension table as possible while still maintaining the full soil core in the frame.

Soil cores were saturated with tap water for 24 hours prior to the experiment. The bottom of the soil core was fitted with cheese cloth to retain soil during saturation. It is

important to saturate the cores from the bottom up to ensure all soil pores become filled with water and all air is expressed. While the soil cores are saturating, the tension table can be prepared per Dane and Hopmans (2002). The tension table should be set to -3.33 cm (Waltz Jr. et al. 2003). A bentonite clay slurry was used to prevent rapid, preferential edge flow from occurring (Blanco-Canqui et al. 2002). The consistency of the slurry is highly dependent on the type of soil. A preliminary study was performed to determine the ratio that would resist preferential edge flow but not hinder water percolation. For this high input turfgrass system a ratio of 1:7 was used.

Once the soil cores have saturated for 24 hours set the core in the center of the tension table, directly above the hole that applies tension. Next, quickly apply water to the top of the core. Allow this water to infiltrate while making sure the core is as straight as possible and is fully captured by the cameras. A straight soil core and quality image are crucial for image processing. When the water has infiltrated, but still saturating the surface, apply the bentonite clay slurry to the interface of the soil surface and cylinder wall.

Immediately after applying the clay slurry, start recording with time lapse photography. For this experiment, the time lapse was set to take one picture every two seconds. Pour 5 cm head of green fluorescent dye into the applicator and allow dye solution to completely infiltrate into the soil core. When infiltration and percolation have ceased, stop recording. Once finished, the soil core may be cut open to visually examine internal flow paths.
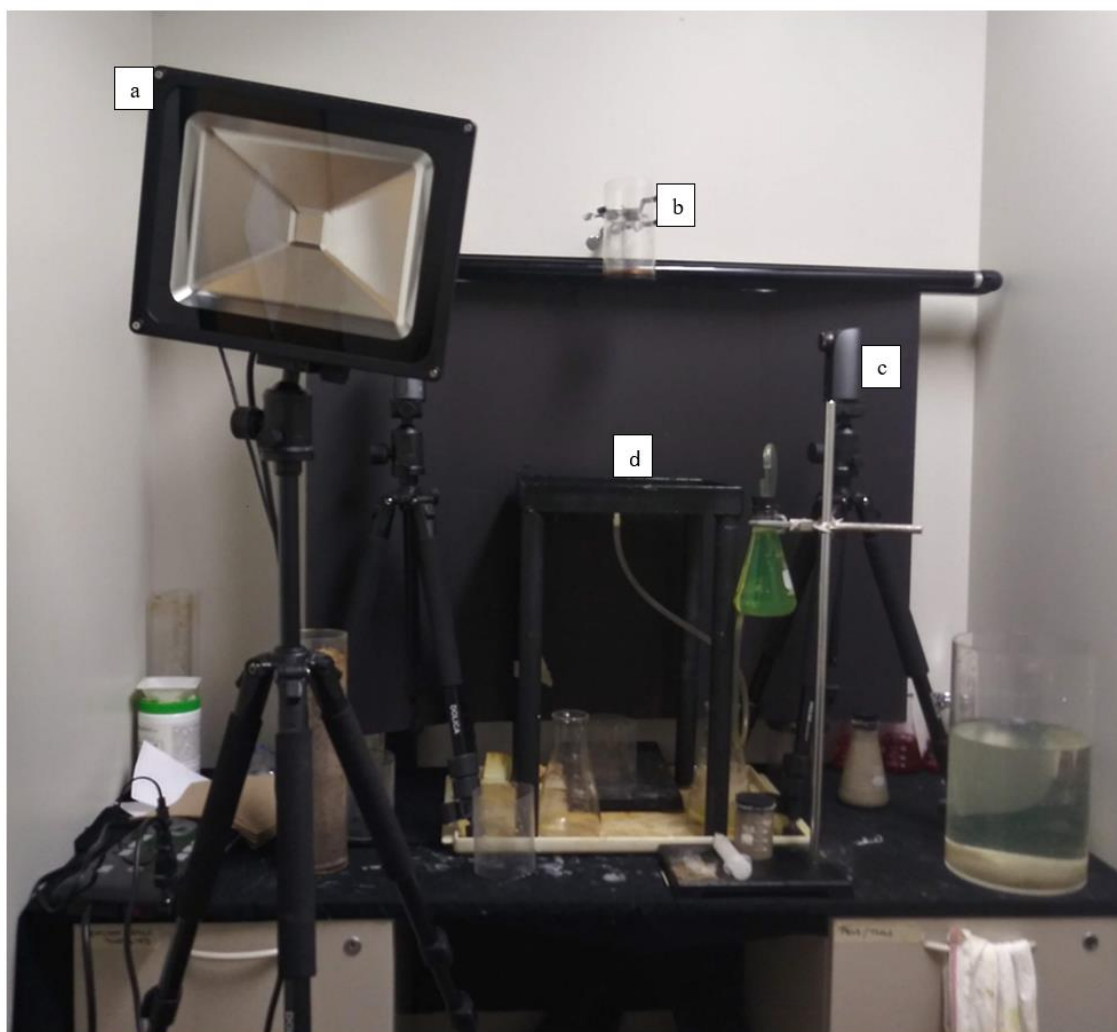
Figure 9. Picture of the dark room used for dye tracing experiments located at the University of Nebraska, Lincoln. The small, windowless room consisted of a a) black light, b) dye applicator, c) time lapse camera on left and right side of tension table, and a d) tension table to apply -3.33 cm to the bottom of the core.
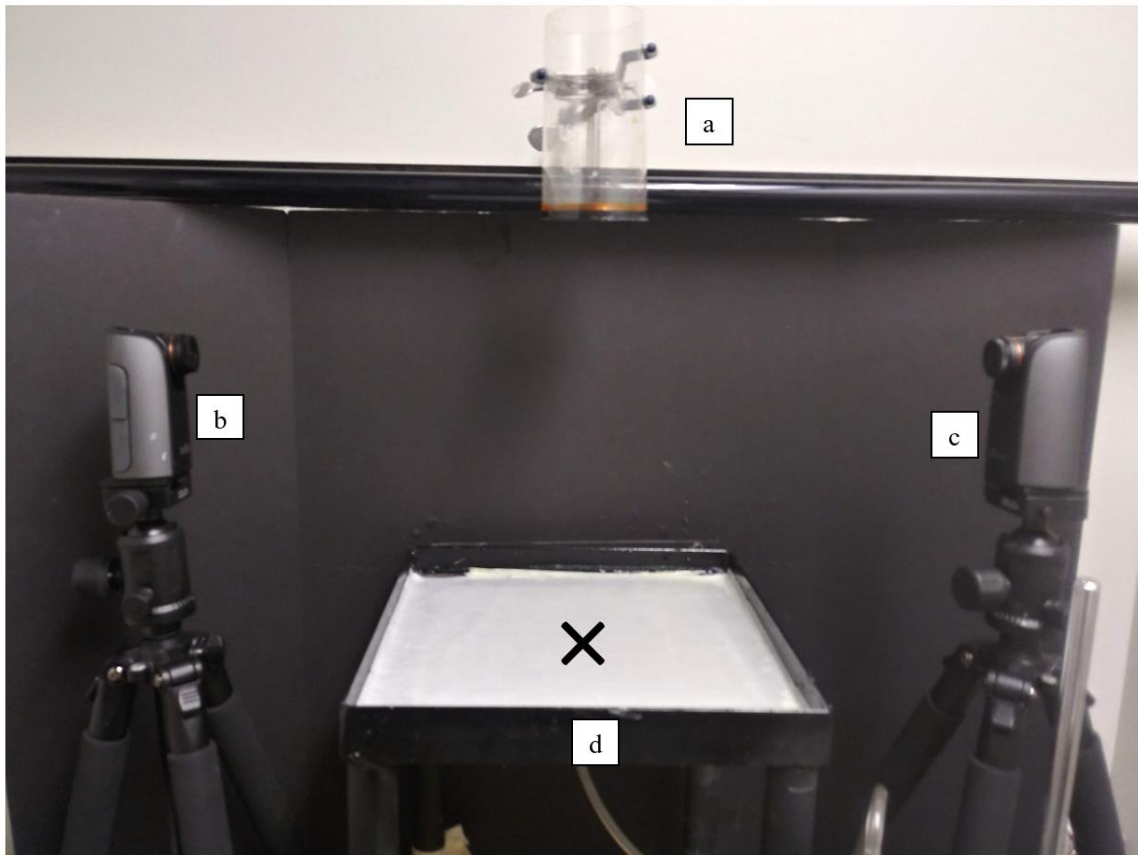
Figure 10. Close up image of the a) dye applicator, b) left side time lapse camera, c) right side time lapse camera, and d) tension table in the dark room used for dye tracing experiments at the University of Nebraska, Lincoln. The 'x' marks the spot where the soil core would sit during dye tracing.

Image Processing and Analysis

Images were processed and analyzed with MATLAB R2021a (MATLAB, Natik, MA). Important parameters such as number of frames, frame height and frame width were defined according to the video camera configuration. The video stream was read into MATLAB as a 4-D numeric array consisting of the red, green and blue (RGB) bands of each frame and the frame dimensions. The first image frame, with no fluorescent signal, was extracted and used as a reference to define the background. A loop was

created to read individual image frames that were compared to the first reference frame. This is how progression of the wetting front was tracked.

The area of interest was defined by selecting the pixel positions of the top, left corner of the column and creating a rectangle that surrounds the soil core. The area of interest was treated as a binary image. Pixels outside the area of interest were set to zero, and pixels inside were set to one. A pixel threshold was determined that would appropriately follow the wetting front. For example, in this study a threshold of 0.40 was used to indicate that when 40% of a row was green pixels, that row should be defined as the wetting front. This threshold was empirically determined based on a visual analysis of the dye tracing videos where it appeared the wetting front made up 40% of the width of the soil core. This threshold was heuristic in nature and could change depending on the flow pattern of the wetting front for each soil core. The wetting front was associated with the most downward point of water movement (Bauters et al. 1998).

The first step of image analysis was to extract the Red (R), Green (G) and Blue (B) bands from the image. Next, an excessive greenness index (ExG, defined as $(2 \times G - R - B) / (R + G + B)$) was calculated. ExG was widely used in image processing applications in agriculture to segment green fresh vegetation from a complex background (Ge et al., 2016, Yuan et al., 2019). In this research, it was found that ExG was also effective in identifying the green, fluorescent pixels. An empirically-determined threshold on 1.0 was used to segment the ExG image into a binary image, with white pixels representing green, fluorescent pixels and black pixels as background. Similar to the wetting front threshold, the ExG threshold was also heuristic in nature and could

change depending on the intensity of the green, fluorescent dye for each soil core. The last step of image analysis was to use row summing to count the number of pixels in each row to determine if it met the threshold used to define the wetting front. A loop was created to read each image frame and tack the movement of the wetting front.

The wetting front position as a function of frame number can be used to estimate the flow rate. The change in pixels from frame to frame represents the length of downward diffusion. The pixel-based metric can be converted to a length based metric using a calibration factor (Equation 1). Multiply the change in pixels by the calibration factor to obtain a length in mm. However, this is the length of downward diffusion for .033 (or 1/30) seconds, because the video rate is 30 frames per second. The length of downward diffusion must be multiplied by 30. This result is the length of downward diffusion in mm sec^{-1}, or flow rate.

Equation 1.

$$Calibration\ Factor = \frac{True\ height\ of\ object\ in\ frame\ (mm)}{Height\ in\ pixels\ of\ object\ in\ frame}$$

Soil Resistance Data

Soil resistance data was collected in the field during sampling. A LC202-5K load cell sensor (Omega, Norwalk, CT) mounted to the tip of the actuator recorded the applied force in compression (pushing the soil core into the ground) and tension (removing the soil sample from the ground). Measurements were made in real time and were reported in

units of pounds of force. The measurements were converted from pound-force to mega

pascals (MPa) for analysis.

Statistical and Data Analysis

Percolation rate data collected from the left and right side of the soil core were

combined to form one data set. This was done because spatial variability of soil physical

properties decreases as samples are taken in closer proximity to one another (Awal et al.,

2019), especially on golf course putting greens with uniform, sandy soil profiles.

Measurements for percolation rate and force were taken in real-time. There was

no set time or depth interval for which each measurement was taken. Therefore, to

compare force and percolation rate measurements, each data set was transformed so that

only observations with both percolation rate and force measurements were used for

analysis. This transformation was performed in SAS 9.4 (SAS Institute, Cary, NC) with

PROC SORT and PROC MEANS functions. First, working with two separate data sets,

each depth measurement was rounded up to the nearest tenth and the mean was calculated

for rate and force values. Next, the two datasets were merged for rate and force by

combining them across location, replicate and rounded depth. Finally, a version of the

combined dataset that removes all observations that do not have both rate and force

measurements was created.

Data was analyzed in SAS with PROC GLIMMIX. Regression analysis was

conducted on percolation rate vs depth and force vs depth. Depth and location were

treated as fixed effects and a random statement was included for variability among

replications. For both soil resistance and rate data, initial models were fit up to a third order polynomial of depth, with interactions included to evaluate if there were significantly different linear, quadratic, or cubic slopes across the locations. An individual location effect was included to test for significantly different intercept values. Terms were determined to be significant at $p \leq 0.05$, and terms that were not significant were removed from the model.

Final models for soil resistance and percolation rate had significant slopes up to cubic ($depth^3$) term. The soil resistance model had significantly different slopes and intercepts across the linear, quadratic, and cubic terms. For the percolation rate models, only the intercept and linear slopes were significantly different across locations. Therefore, slopes for the quadratic ($depth^2$) and cubic ($depth^3$) terms were the same for the three percolation rate regression lines. The regression equations used for soil resistance are shown in Equation 2 and the equations used for percolation rate are shown in Equation 3.

Equation 2.

$$\widehat{Predicted\ Force}_{East\ Campus} = -275.50 + 182 * DepthRound + 0.7140 * DepthRound^2 - 0.1279 * DepthRound^3$$

$$\widehat{Predicted\ Force}_{Holmes} = -176.58 + 181.31 * DepthRound - 3.5039 * DepthRound^2 + 0.1113 * DepthRound^3$$

$$\widehat{Predicted\ Force}_{Mahoney} = -87.6177 + 89.4375 * DepthRound + 5.3245 * DepthRound^2 - 0.1595 * DepthRound^3$$

Equation 3.

$$\widehat{Predicted\ Rate}_{East\ Campus} = 41.4426 + 8.3821 * DepthRound - 0.7861 * DepthRound^2 + 0.01644 * DepthRound^3$$

$$\widehat{Predicted\ Rate}_{Holmes} = 10.5060 + 10.3241 * DepthRound - 0.7861 * DepthRound^2 + 0.01644 * DepthRound^3$$

$$\widehat{Predicted\ Rate}_{Mahoney} = 17.5632\ + 9.3883 * DepthRound - 0.7861 * DepthRound^2 + 0.01644 * DepthRound^3$$

The R^2 value for each data set was calculated in SAS with PROC IML. The

adjusted R^2 value was used for analysis because there are additional polynomial terms

that fit beyond linear. The adjusted R^2 values were calculated using Equation 4.

Differences between locations were examined by testing significance in 2.5 cm

increments.

Equation 4.

$$R^2_{adj} = 1 - (1 - R^2)\frac{n - 1}{n - p - 1}$$

Where n = number of observations, and p = number of coefficients in regression
models.

RESULTS AND DISCUSSION

Visualizing Water Movement in Modified Root Zones

Figures 11-13 show screen captures documenting the progression of the wetting

front for all 5 replications (reps) at each location. The dye patterns in the images illustrate

the variability of water movement in golf course putting greens, as no two reps displayed

the same flow patterns, even within the same location. The flow patterns of the left and

right sides of the soil core for each replication were similar to one another in the depths

reached by the dye and in the areas that resisted wetting. Flow paths visualized were

continuous down the length of the soil core. This is in agreement with Shein et al. (2009)

who noted similar uninterrupted flow paths in sandy soils.

Similar to previous dye tracing experiments in sand dominated soils, dye coverage decreased with depth in all soil cores, at all locations (Nektarios et al. 2007, Zhang et al. 2021). The depth reached by the dye at the end of the experiment was similar for all locations. The depth of dye reached in this study ranged from 20-27 cm. This matches the depth reached in dye tracing experiments (22-27 cm) reported by Nektarios et al. (2007) under various aeration treatments in golf course putting greens.

Preferential flow was visible at all locations and finger flow formation was visible in the top 15 cm. There were two or three distinct finger paths that developed in the soil cores at each location. In soils with high sand content and poor structure, the wetting front may become unstable and thin finger flow paths start to form (Flury and Fluhler 1994). Typically, greater initial water content, especially in sandy soils, creates a more stable wetting front (Geiger and Dunford 2000, Merdun et al. 2008, Gerke et al. 2015). Using saturated soil cores could explain the formation of only a few finger flow paths in each replication.

East Campus

Left   Right

Figure 11. Screen shots of the progression of the wetting front for the left and right sides of replication (rep) 1-5 at East Campus research plots at the University of Nebraska in Lincoln, Ne. Scale is in centimeters.

Figure 12. Screen shots of the progression of the wetting front for the left and right sides of replication (rep) 1-5 at Holmes golf course in Lincoln, Ne. Scale is in centimeters.

Mahoney

Left   Right

Figure 13. Screen shots of the progression of the wetting front for the left and right sides of replication (rep) 1-5 at Mahoney golf course in Lincoln, Ne. Scale is in centimeters.

Rapid, finger flow has been widely reported in golf course putting greens (Nektarios et al. 2002, Nektarios et al. 2007, Larsbo et al. 2008, Song et al. 2014,). In turf systems preferential flow paths can develop from water repellant sands, soil layer formation, and/or macropores created after aeration events that expose soil to the surface creating rapid points of entry for infiltrating water (Hill and Parlange 1972, Nektarios et al. 2002, Nektarios et al. 2007, Allaire et al. 2009). Nektarios et al. (2002) stated finger-flow was in fact the primary mechanism for water movement in USGA putting green profiles. Similarly, Flury et al. (1994) suggested that in poorly structured, sandy soils the presence of preferential flow paths is often seen as the rule rather than the exception.

As infiltration progressed, finger paths that started very thin widened out and became less pronounced. At the end of the dye tracing experiment some preferential finger paths were no longer visible. Furthermore, some areas that resisted wetting during initial infiltration, became wetted as infiltration progressed and were no longer visible at the end of the dye tracing experiment. Yet, the deepest depths reached by the dye was still from quick moving preferential flow paths.

Rapid water movement through large macropores dominated the beginning of water infiltration into the putting greens. As infiltration continues, horizontal movement of water starts to enlarge finger size (Kawamoto et al. 2004) and smaller pores in the bulk of the soil matrix start to absorb water (Schneider et al. 2018), especially in the top soil. This masks the finger flow paths that were visible early during infiltration, resulting in the appearance of a uniformly saturated soil profile at the end of the dye tracing experiment, especially in the 0-15 cm depths. Similar to this study, Zhang et al. (2021)

also found that soil matrix flow contributed to more dye staining towards the surface compared to preferential flow paths. Water movement in soils has been said to be a combination of soil matrix flow and preferential flow (Legout et al. 2009, Zhang et al. 2016).

The dye patterns visualized in this study are similar to those reported in other studies for sand based soils (Morris and Mooney 2003, Nektarios et al. 2007, Kodesova et al. 2011, Lichner et al. 2011). The dye patterns visualized in this study are contrasting with those reported by Mossadeghi-Bjorkland et al. (2018) for a clay soil that displayed predominantly preferential flow and very little soil matrix infiltration. Such stark differences would be expected due to differences in soil texture between the two studies.

East Campus displayed the most uniform wetting front among all three locations (Figure 11). The more uniform wetting front at East Campus is likely a result of frequent aeration and topdressing events that have increased soil macroporosity. It is known that frequent aeration and topdressing events can improve water movement in golf course putting greens (Sorokovsky et al. 2006, Nektarios et al. 2007, Schmid et al. 2014, Craft et al. 2016).

In all East Campus reps, infiltration in the top 0-2.5 cm was very uniform. However, at Holmes and Mahoney finger flow was visible starting from initial infiltration (0-2.5 cm). Preferential flow paths forming near the surface is a result of water flowing through macropores in a hydrophobic organic layer (Schneider et al. 2018). This refers to the thatch mat layer in turfgrass systems which has been shown to inhibit water infiltration and initial percolation (Gaussoin et al. 2013, Schmid et al. 2014).

Hydrophobic soil surfaces often produce unstable wetting fronts leading to water movement via preferential flow paths (Bauters et al. 1998, Kim et al. 2005, Nektarios et al. 2007)

In all replications at Holmes there was an area that resisted wetting at 17-20 cm. It is possible a hardened layer formed from repetitive aeration events at a consistent depth. Over time, this hardened layer may become too compact and resist water infiltration (Brye et al. 2005). Mossadeghi-Bjorkland et al. (2018) also reported an area in the subsoil (20-30 cm) that resisted infiltration that they attributed to a compaction layer. Lateral flow was visible in reps 1,2, and 3 (Figure 12). Lateral flow was characterized by flow patterns that appeared to sweep across the soil core and move more horizontally than vertically. These were the only soil cores that displayed this type of flow pattern.

All soil cores were cut open after dye tracing experiment to examine internal flow paths and assess if preferential edge flow had occurred (Figure 14). Preferential edge flow is an artifact of poor soil sampling when the soil sample and cylinder wall are not in close contact. Flow patterns indicative of preferential edge flow are deep flow paths concentrated near the cylinder walls with very little dye infiltration in the center of the core. A visual assessment showed that no preferential edge flow occurred in the soil cores (Figure 14).

Some flow paths were visible on the inside of the soil core that were not visible on the outside wall. Further discrediting the possibility of preferential edge flow. Similar flow paths that resisted contact with the cylinder wall were reported by Hill and Parlange (1972). Many of the soil cores displayed internal finger flow paths, a few centimeters

wide, indicating preferential flow via holes made by aeration tines. This was especially evident in Holmes rep 4 (Figure 12). Nektarios et al. (2007) also noted similar stained finger flow paths caused by aeration holes after dye tracing experiments.

Calculate a Rate Based on the Movement of the Wetting Front

A flow rate was able to be calculated in mm sec^{-1} based on the advancement of the wetting front. Table 2 shows predicted rates based on the regression analysis equations for each location. The flow rates calculated at 2.5 cm increments for 30 cm depth, ranged from 20.06 to 67.23 mm sec^{-1} (Table 2). There were statistical differences among locations in the top 0-20 cm only. East Campus had significantly higher flow rates compared to Holmes. Mahoney was not statistically different from Holmes or East Campus.

Regression analysis showed flow rate was not correlated with depth ($R^2_{adj.} =$ 0.152). Factors such as soil structure, texture (root zone composition), and organic matter content influence particle size distribution and pore characteristics and play a greater role in water movement throughout the profile compared to depth sampled (Bigelow and Soldat 2013).

At each depth calculated, East Campus always had the highest flow rates (Figure 15). For all locations, the lowest flow rate was in the 0-2.5 cm depth (Table 2). Organic matter in the thatch layer has been shown to inhibit water infiltration and initial percolation (Schmid et al. 2014, Gaussoin et al. 2013). For all locations, the

East Campus
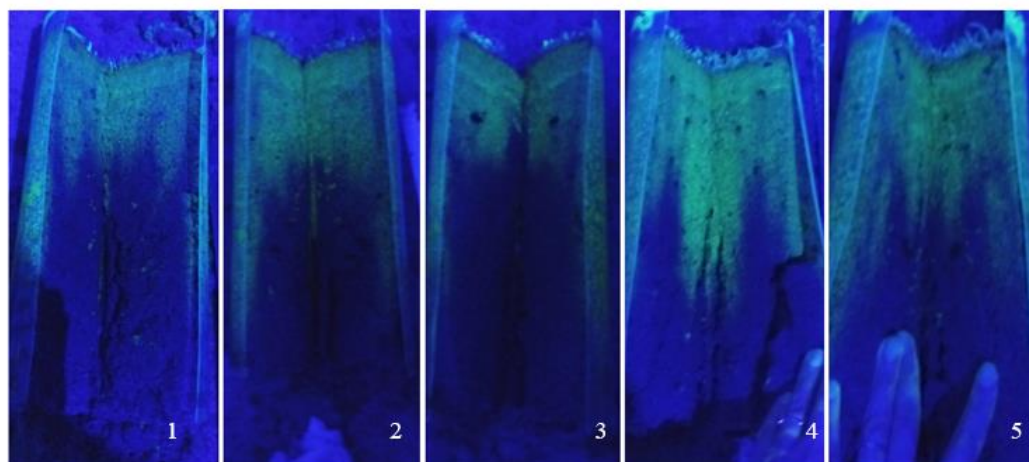
Holmes
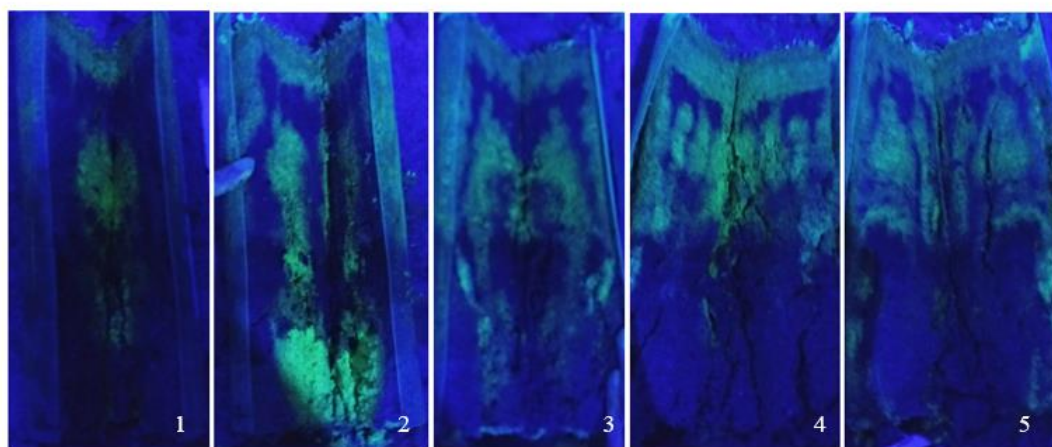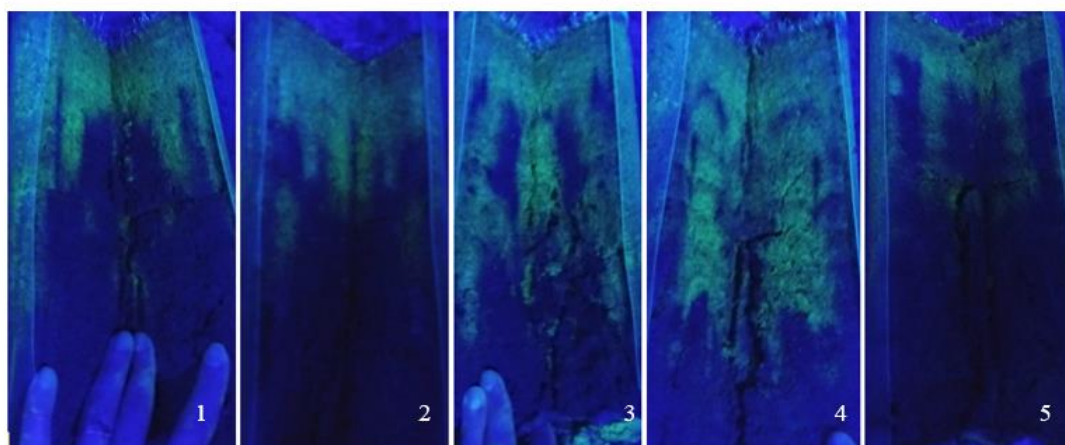
Mahoney

Figure 14. After the dye tracing experiment soil cores were cut open to examine internal flow paths for all locations- East Campus, Holmes, and Mahoney, and for all replications 1-5 (indicated in the corner of each picture).

highest rate was between 18-23 cm (Table 2). This depth corresponds to the area just below depth of aeration, where a hardpan layer is likely to form. The quick water movement at this depth represents the breakthrough of water past the hardened layer.

There was a greater increase in flow rate from 0-15 cm compared to the decrease in rate from 15-30 cm. The large increases in flow from centimeter to centimeter indicates an area of quick water movement that is a direct result from aerification of the upper 15 cm. The process of physically opening the soil surface with aeration, combined with frequent topdressing applications, reduces bulk density and increases porosity which improves water movement (Rowland et al. 2009, Gaussoin et al. 2013).

This method may prove useful in quantifying preferential flow rates, which is a measurement that has classically been inferred (Allaire et al. 2009). No other study has been found that has attempted to calculate a percolation rate based on the real-time advancement of the wetting front. Therefore, no previous rates exist to compare with the rates calculated in this study. Future research should be done using an established method of calculating infiltration rates (i.e., saturated hydraulic conductivity) with the same 30 cm soil cores used in this study to correlate measured rates to determine validity of this method.

Figure 15. Regression analysis for flow rate by depth for three golf course putting greens in Lincoln, Ne. Adjusted R^2 value is 0.152 for this analysis.

Table 2. Water flow rate measurements for three putting greens in Lincoln, NE. Letters indicate significant differences across locations at p=<0.05.

Depth (cm)	East Campus	Holmes	Mahoney
	Flow Rate (mm sec^{-1})		
2.5	49.05a	20.06b	26.18ab
5	55.19a	28.14b	33.32ab
7.5	59.95a	34.84b	39.09ab
10	63.44a	40.27b	43.59ab
12.5	65.76a	44.52b	46.90ab
15	66.98a	47.70b	49.14ab
17.5	67.23a	49.89b	50.40ab
20	66.60a	51.20b	50.77ab
22.5	65.19	51.73	50.37
25	63.09	51.57	49.27
27.5	60.41	50.83	47.6
30	57.24	49.61	45.43

Soil Resistance

Results for soil resistance measurements are in Table 3. There was an increase in cumulative force with depth at all locations (Figure 16). Location was highly significant for all interactions. Regression analysis showed resistance was highly correlated with depth ($R^2_{adj.}$ = 0.976). This agrees with previous research that shows as profile depth increases, so does the force required to penetrate the soil (Carter 1988, Mossadeghi-Bjorklund et al. 2018, Fashi et al. 2019).

Across all locations, soil resistance remained below 0.30 MPa in the top 0-5 cm (Table 3). These measurements are similar to those recorded by de Koff et al. 2010 for compost mixed with waste foundry sand. Similarities indicate a layer of high organic content. In turf systems this is referred to as the thatch mat layer and it is characterized by its high organic matter content (Gaussoin et al. 2013). Organic matter is also known to decrease soil bulk density (Raturi et al. 2005, Stock and Downes 2008), which is often an indicator of the soils resistance to penetration (Hernanz et al. 2000).

There were no differences among location from 0-15 cm (Table 3). The putting greens at all locations are aerated several times a year and this common management practice may have created similar conditions in the top 0-15 cm resulting in very similar resistance measurements for all locations.
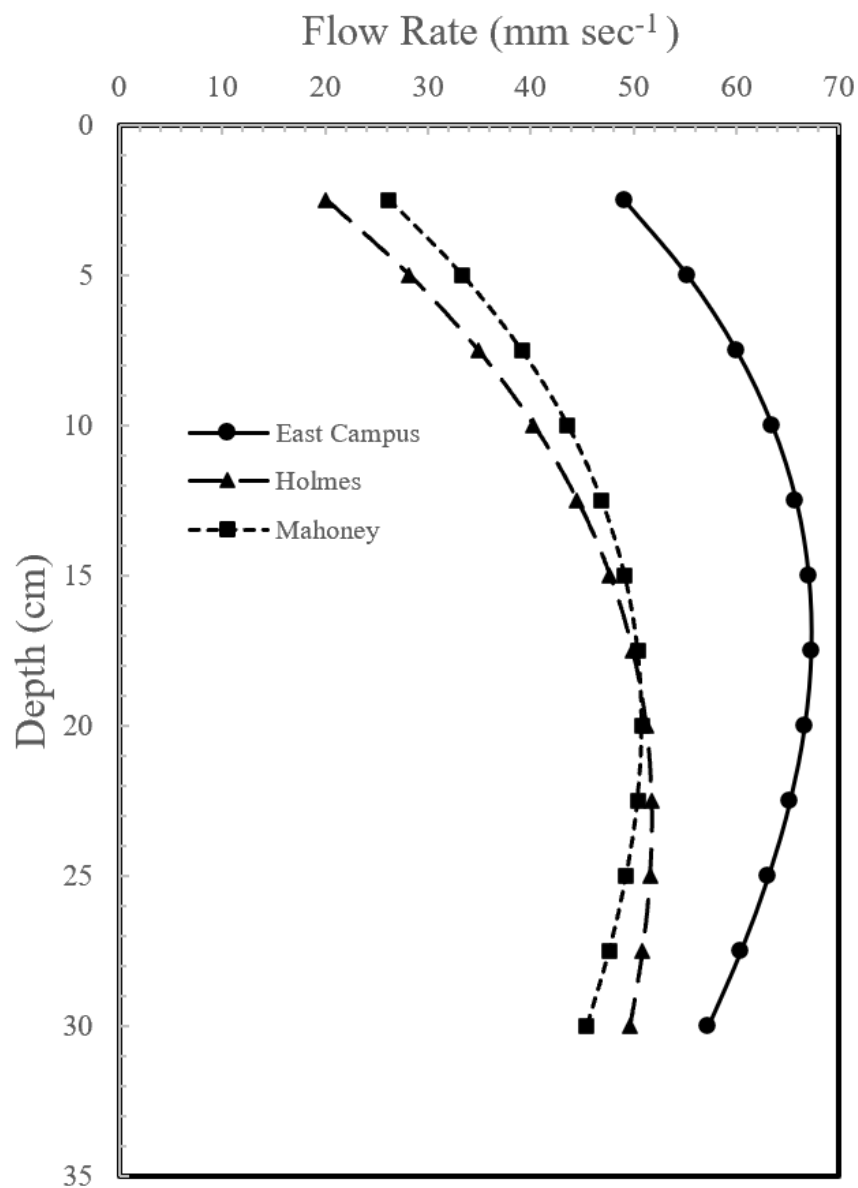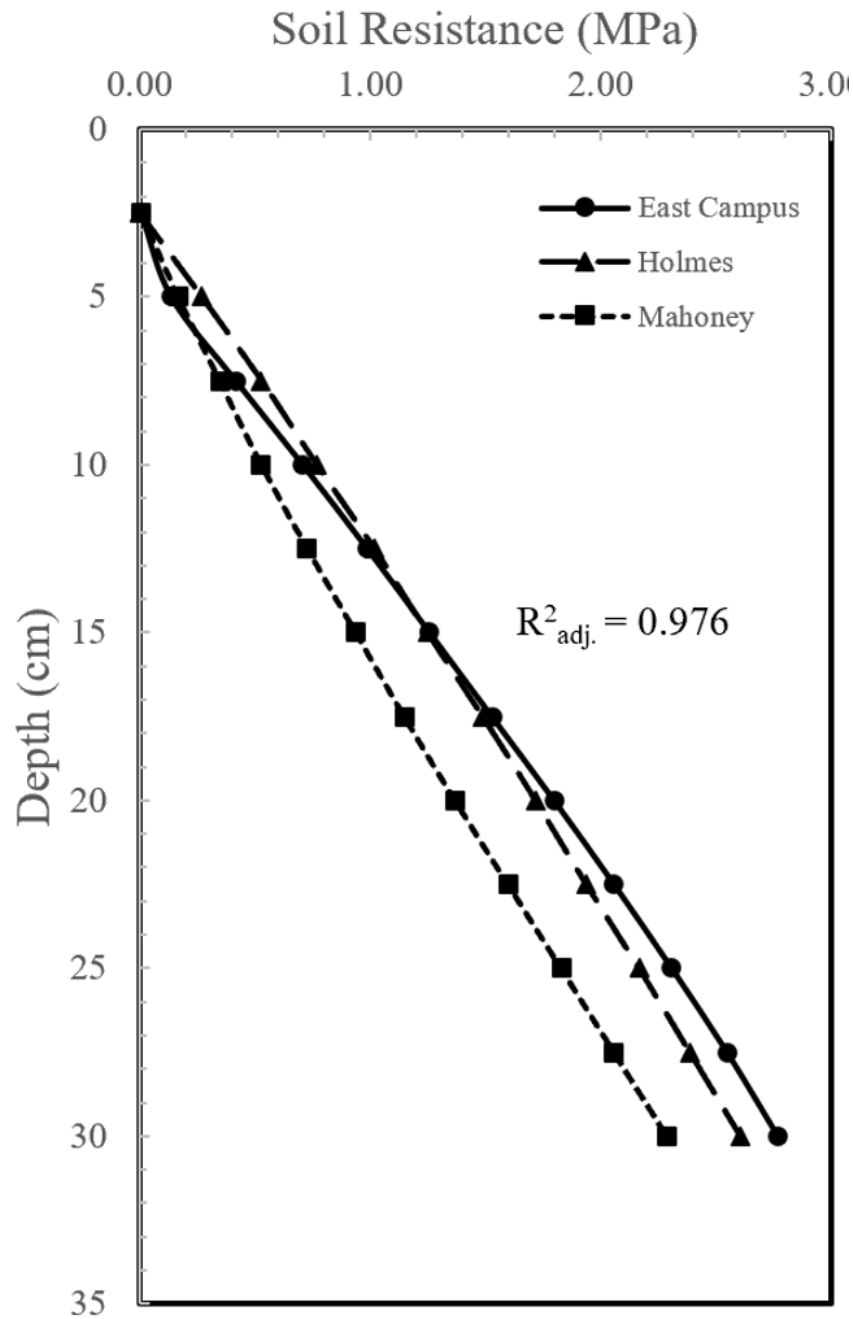
Figure 16. Regression analysis for soil resistance by depth for three golf course putting greens in Lincoln, Ne. Adjusted R^2 is 0.976 for this analysis.

Table 3. Soil resistance measurements for three putting greens in Lincoln, NE. Letters indicate significant differences across locations at p=<.05.

	Soil Resistance (MPa)		
Depth (cm)	East Campus	Holmes	Mahoney
2.5	0.01	0.00	0.01
5	0.14	0.27	0.17
7.5	0.42	0.53	0.35
10	0.71	0.77	0.53
12.5	0.99	1.02	0.73
15	1.26a	1.25a	0.94b
17.5	1.53a	1.49a	1.15b
20	1.80a	1.72a	1.37b
22.5	2.06a	1.94a	1.60b
25	2.31a	2.17a	1.83b
27.5	2.55a	2.39a	2.06b
30	2.77a	2.61a	2.29b

There were significant differences among locations from 15-30 cm (Table 3). This is comparable to Alaoui and Diserens (2011), who reported no significance from 0-10 cm, but found differences from the 10-30 cm depth. Mahoney golf course had significantly lower force in the bottom half of the soil profile compared to East Campus and Holmes. There were no significant differences between East Campus and Holmes. It is possible that a hard pan has formed on the greens at East Campus and Holmes which is causing the higher force needed to penetrate the soil at 15 cm. Hard pans form from repetitive soil disturbance to a consistent depth and have been shown to hinder water movement through the profile resulting in poor plant growth (Tekeste et al. 2008). Increased aeration events at East Campus could have caused greater soil compaction.

Mahoney had 25% lower soil resistance at 15 cm compared to East Campus and Holmes. While at 30 cm Mahoney had only 15% lower resistance compared to East Campus and Holmes. The decrease in percent difference as you move from 15 cm to 30 cm further supports the theory of a hard pan layer formation at East Campus and Holmes. As depth increases past the hardened layer, the effects begin to dissipate and soil physical properties become more homogeneous.

The resistance measurements collected in this study agree with previous studies. At 15 cm, the measured resistance is similar to that measured by Glab and Szewczyk (2014) for the nontrafficked mean of various golf course turfgrass species. Resistance measured in the putting greens are lower than those measured by Mossadeghi-Bjorkland et al. (2018) for compacted agricultural soils. Resistance into sandy, uniform putting

green profiles would be expected to be lower due to the greater resistance of sand particles to compaction.

The advantages and weaknesses of this method compared to previous methods will now be discussed. This method could prove useful for such applications as identifying soil layer formation, understanding how water movement changes over time, and quantifying preferential water flow. The main advantage of this method is the ability to visualize water movement in soils that cannot be excavated, such as modified root zones or soils in urban environments. This method also allows a real-time visualization of water infiltration and percolation which allows a more precise evaluation of flow path formation and evolution during water infiltration. Information of this nature would provide a better understanding of water exchange between preferential flow paths and the soil matrix.

A weakness of this method is the inability to visualize internal flow paths. If these flow paths cannot be captured with time lapse photography, then a flow rate cannot be calculated. Flow rates calculated are only for the part of the soil core that is visible through the transparent cylinder wall. Also, this method has not been tested in soils with clay and silt contents typical of native soils. It is not known how this method would work for these types of soils. Further work should be done to assess the suitability of this method for a variety of soil types. Future research should also be done to calibrate flow rates with those calculated with a known infiltration method (i.e. saturated hydraulic conductivity). Lastly, the soil sampler could be further improved to include soil moisture sensors, providing a more in depth analysis into soil resistance and water movement.

CONCLUSION

The method described here is a useful method for visualizing water movement through modified, sand based root zones. Using undisturbed soil cores 30 cm in length flow paths were illuminated with green, fluorescent dye and UV light and captured with time lapse photography. The flow patterns captured in this study illustrate the quick initial movement of water through preferential pathways and the slower absorption of micropores as infiltration progresses.

Using MATLAB software, the movement of the wetting front was tracked. A flow rate was calculated based on the change in dye pixels from frame to frame. Rates calculated were very high and are likely characteristic of preferential flow and not flow through the soil matrix. Further research should be done to validate flow rates calculated with this method. The ability to measure soil resistance while simultaneously removing a soil sample proved a useful tool in understanding water movement in golf course putting greens. Soil resistance measured in this study corresponded well with those of previous studies.

This method has the potential to provide quality information on water movement in modified root zones including flow path development and evolution over time, monitor changes in soil layering, and quantifying flow rates. This method could be used to better the understanding of how management practices such as aeration techniques, topdressing applications, and surfactant use influence water movement and flow path development in golf course putting greens.

REFERENCES

Alaoui, A., and E. Diserens. 2011. Changes in soil structure following passage of a tracked heavy machine. Geoderma. 163: 283-290.

Allaire. S.E., S. Roulier, and A.J. Cessna. 2009. Quantifying preferential flow in soils. A review of different techniques. Journal of Hydrology. 378: 179-204.

Anderson, A.E., M. Weiler, Y. Alila, and R. O. Hudson. 2008. Dye staining and excavation of a lateral preferential flow network. Hydrology and Earth System Sciences Discussions. 5(2): 1043-1065.

Armson, D., P. Stringer, and A.R. Ennos. 2013. The effect of street trees and amenity grass on urban surface water runoff in Manchester, UK. Urban Forestry and Urban Greening. 12: 282-286.

ASTM. 2003. (ASTM D 3385) Standard test method for infiltration rate of soils in field using double-ring infiltrometer. ASTM International.

Awal, R., M. Safeeq, F. Abbas, S. Fares, S.K. Deb, A. Ahmad, and A. Fares. 2019. Soil physical properties spatial variability under long-term no-tillage corn. Agronomy. doi:10.3390/agronomy9110750.

Babaei, F., A.A. Zolfaghari, M.R. Yazdani, A. Sadeghipour. 2018. Spatial analysis of infiltration in agricultural lands in arid areas of Iran. Catena. 170: 25-35.

Bauters, T.W.J., D.A. DiCarlo, T.S. Steenhuis, and J.Y. Parlange. 1998. Preferential flow in water-repellant sand. Soil Science Society of America Journal. 62: 1185-1190.

Berndt, W.L. 2016. Redox potential and black layer. Golf Course Management. 6: 86-91.

Bevard, D.S. 2009. Water, water everywhere! Green Section Record. p.4-6.

Bigelow, C.A., D.C. Bowman, and D.K. Cassel. 2001. Water retention of sand-based putting green mixtures as affected by the presence of gravel sub-layers. International Turfgrass Society Research Journal. 9: 479-486.

Bigelow, C.A. and D.J. Soldat. 2013. Turfgrass root zones: management, construction methods, amendment characterization, and use. In J.C. Stier et al. (Eds.), Turfgrass: Biology, Use, and Management. pp 383-423. ASA, CSSA, and SSSA

Blanco-Canqui, H., C.J. Gantzer, S.H. Anderson, E.E. Alberts, and F. Ghidey. 2002. Saturated hydraulic conductivity and its impact on simulated runoff for claypan soils. Soil Science Society of America Journal. 66: 1596-1602.

Brye, K.R., N.A. Slaton, and R.J. Norman. 2005. Penetration resistance as affected by shallow-cut land leveling and cropping. Soil & Tillage Research. 81:1-13.

Carrillo, M.L.K., J. Letey, and S.R. Yates. 2000. Unstable water flow in a layered soil: I. Effects of a stable water-repellant layer. Soil Science Society of America Journal. 64:450-455.

Carter, M.R. 1988. Penetration resistance to characterize the depth and persistence of soil loosening in tillage studies. Canadian Journal of Soil Science. 68: 657-668.

Clothier, B.E., S.R. Green, and M. Deurer. 2008. Preferential flow and transport in soil: progress and prognosis. European Journal of Soil Science. 59: 2-13.

Cockerham, S.T., B. Leinauer, P.E. Reike, J.A. Murphy, and R. Green. 2012. Turfgrass water conservation essentials: modified rootzones and current water management technologies. Sports Turf. p. 12-15.

Craft, J.M., C.M. Baldwin, W.H. Philley, J.D. McCurdy, B.R. Stewart, M. Tomaso-Peterson, and E.K. Blythe. 2016. Impact of dry-injection cultivation to maintain soil physical properties for an ultradwarf bermudagrass putting green. HortScience. 51(9):1171-1175.

Dane, J.H., and J.H. Hopmans. 2002. Water retention and storage. In: J.H. Dane and G.C. Topp, editors, Methods of soil analysis. Part 4. Agron. Monogr. 5. SSSA, Madison, WI. p. 671–717.

Dekker, L.W., K. Oostindie, A.K. Ziogas, and C.J. Ritsema. 2001. The impact of water repellancy on soil moisture variability and preferential flow. International Turfgrass Society Research Journal. 9:498-505.

DePew, M., and S. Guise. 2001. Engineered soils for sports field constructions. Sports Turf. p.32-35.

Fashi, F.H., M. Gorji, and F. Sharifi. 2019. Temporal variability of soil water content and penetration resistance under different soil management practices. Journal of Soil and Water Conservation. 74: 188-198.

Feuki, N., J. Lipiec, J. Kus, U. Kotowska, and A. Nosalewicz. 2012. Difference in infiltration and macropore between organic and conventional soil management. Soil Science and Plant Nutrition. 58: 65-69.

Filipovic, V., G.S. Toor, G. Ondrasek, and R. Kodesova. 2015. Modeling water flow and nitrate-nitrogen transport on golf course under turfgrass.

Fisher, M. 2017. Soil evolution: Par for the golf course. CSA News. p. 4-7

Flury, M. and H. Fluhler. 1994. Susceptibility of soils to preferential flow of water: A field study. Water Resources Research. 30: 1945-1954.

Flury, M., H. Fluhler, W.A. Jury, and J. Leuenberger. 1994. Susceptibility of soils to preferential flow of water: A field study. Water Resources Research. 30(7):1945-1954.

Gaussoin, R., R. Shearman, L. Wit, T. McClellan, and J. Lewis. 2007. Soil physical and chemical characteristics of aging golf greens. Golf Course Management. p. 161-165.

Gaussoin, R., W.L. Berndt, C.A. Dockrell, and R.A. Drijber. 2013. Characterization, development, and management of organic matter in turfgrass systems. In Turfgrass: Biology, Use, and Management. p. 425-456.

Ge, Y., G. Bai, V. Stoerger, and J.C. Schnable. 2016. Temporal dynamics of maize plant growth, water use, and leaf water content using automated high throughput RGB and hyperspectral imaging. Computers and Electronics in Agriculture. 127: 652:632.

Geiger, S.L. and D.S. Dunford. 2000. Infiltration in homogeneous sands and a mechanistic model of unstable flow. Soil Science Society of America Journal. 64: 460-469.

Gerke, K.M., R.C. Sidle, and D. Mallants. 2015. Preferential flow mechanisms identified from staining experiments in forested hillslopes. Hydrological Processes. 29: 4562-4578.

Glab, T. and W. Szewczyk. 2014. Influence of simulated traffic and roots of turfgrass species on soil pore characteristics. Geoderma. 230-231: 221-228.

Hamilton, G.W. and D.V. Waddington. 1999. Infiltration rates on residential lawn in central Pennsylvania. Journal of Soil and Water Conservation. 54: 564-568.

Hassan, G., R. Reneau, and C. Hagedorn. 2010. Solute transport dynamics where highly treated effluent is applied to soil at varying rates and dosing frequencies. Soil Science. 175: 278-292.

Hassanpour, B., B. K. Richards, L.D. Goehring, J.Y. Parlange, and T.S. Steenhuis. 2019. Predicting the fate of preferentially moving herbicides. Vadose Zone Journal. 18:180193.

Hendrickz, J.M.H., L.W. Dekker, and O.H. Boersma. 1993. Unstable wetting fronts in water-repellant field soils. Journal of Environmental Quality. 22: 109-118.

Hernanz, J.L., H. Peixoto, C. Cerisola, and V. Sanchez-Giron. 2000. An empirical model to predict soil bulk density profiles in field conditions using penetration resistance, moisture content and soil depth. Journal of Terramechanics. 37: 167-184.

Hill, D.E. and J.Y. Parlange. 1972. Wetting front instability in layered soils. Soil Science Society of America Proceedings. 36(5): 697-702.

Hillel, D. 2004. Water entry into soil. In Introduction to Environmental Soil Physics. Elsevier Science.

Hopmans, J.W., J.Y. Parlange, and S. Assouline. 2017. Infiltration. In The Handbook of Groundwater Engineering. p. 191-202.

Jarvis, N.J. 2007. A review of non-equilibrium water flow and solute transport in soil macropores: principles, controlling factors and consequences for water quality. European Journal of Soil Science. 58: 523-546.

Johnson, A.I. 1963. A field method for measurement of infiltration. Geological Survey Water-Supply Paper 1554-F.

Kaestner, A., E. Lehmann, and M. Stampanoni. 2008. Imaging and image processing in porous media research. Advances in Water Resources. 31: 1174-1187.

Kawamoto, K., S. Mashino, M. Oda, and T. Miyazaki. 2004. Moisture structures of laterally expanding fingering flows in sandy soils. Geoderma. 119: 197-217.

Keestra, S.D., J. Bouma, J. Wallinga, P. Tittonell, P. Smith, A. Cerda, L. Montanarella, J.N. Quinton, Y. Pachepsky, W.H. van der Putten, R.D. Bardgett, S. Moolenaar, G. Mol, B. Jansen, and L.O. Fresco. 2016. The significance of soils and soil science towards realization of the United Nations sustainable development goals. Soil. 2: 111-128.

Kim, Y.J., C.J.G. Darnault, N.O. Baily, J.Y. Parlange, and T.S. Steenhuis. 2005. Equation for describing solute transport in field soils with preferential flow paths. Soil Science Society of America Journal. 69: 1-10.

Kodesova, R., K. Nemecek, V. Kodes, and A. Zigova. 2011. Using dye tracer for visualization of preferential flow at macro- and microscales. Vadose Zone Journal. doi:10.2136/vzj2011.0088.

de Koff, J.P., B.D. Lee, R.S. Dungan, and J.B. Santini. 2010. Effect of compost-, sand-, or gypsum-amended waste foundry sands on turfgrass yield and nutrient content. Journal of Environmental Quality. 39: 376-380.

Kohne, J.M. and B.P. Mohanty. 2005. Water flow processes in a soil column with a cylindrical macropore: Experiment and hierarchical modeling. Water Resources Research. 41: W03010.

Larsbo, M., T.S. Aamlid, L. Persson, and N. Jarvis. 2008. Fungicide leaching from golf greens: Effects of root zone composition and surfactant use. Journal of Environmental Quality. 37: 1527-1535.

Legout, A., C. Legout, C. Nys, and E. Dambrine. 2009. Preferential flow and slow convective shloride transport through the soil of a forested landscape (Fougeres, France). Geoderma. 151: 179-190.

Lewis, J.D., R.E. Gaussoin, R.C. Shearman, M. Mamo and C.S. Wortmann. 2010. Soil physical properties of aging golf course putting greens. Crop Science. 50: 2084-2091.

Lichner, L., D.J. Eldridge, K. Schacht, N. Zhukova, L. Holko, M. Sir, and J. Pecho. 2011. Grass cover influences hydrophysical parameters and heterogeneity of water flow in a sandy soil. Pedosphere. 21(6): 719-729.

Luo, L. and H. Lin. 2009. Lacunarity and fractal analyses of soil macropores and preferential transport using micro-x-ray computed tomography. Vadose Zone Journal. 8: 233-241.

Luo, L., H. Lin, and P. Halleck. 2008. Quantifying soil structure and preferential flow in intact soil using x-ray computed tomography. Soil Science Society of America Journal. 72: 1058-1069.

McCarty, L.B., L.R. Hubbard, Jr., and V. Quisenberry. 2016. Applied soil physical properties, drainage, and irrigation strategies. Springer International.

McCoy, E.L. and K.R. McCoy. 2009. Simulation of putting-green soil water dynamics: Implications for turfgrass water use. Agricultural Water Management. 96: 405-414.

Merdun, H., R. Meral, and A.R. Demirkiran. 2008. Effect of the initial soil moisture content on the spatial distribution of the water retention. Eurasian Soil Science. 41: 1098-1106.

Morris, C., and S.J. Mooney. 2003. A high-resolution system for the quantification of preferential flow in undisturbed soil using observations of tracers. Geoderma. 118: 133-143.

Mossadeghi-Bjorkland, M., N. Jarvis, M. Larsbo, J. Forkman, and T. Keller. 2018. Effects of compaction on soil hydraulic properties, penetration resistance and water flow patterns at the soil profile scale. Soil Use and Management. 35: 367-377.

Nektarios, P.A., A.M. Petrovic, and T.S. Steenhuis. 2002. Effect of surfactant on fingered flow in laboratory golf greens. Soil Science. 167: 572-579.

Nektarios, P.A., A.M. Petrovic, and T.S. Steenhuis. 2007. Preferential flow in simulated greenhouse golf putting greens as affected by aeration and two soil moisture regimes. Soil Science. 172: 108-123.

Nimmo, J.R. 2012. Preferential flow occurs in unsaturated conditions. Hydrological Processes. 26: 786-789.

Noguchi, S., Y. Tsuboyama, R.C. Sidle, and I. Hosoda. 1999. Morphological characteristics of macropores and the distribution of preferential flow pathways in a forested slope segment. Soil Science Society of America Journal. 63: 1413-1423.

Obear, G.R., A.E. Hartemink, and D.J. Soldat. 2014. Soils with iron-cemented layers on golf courses in the USA. Geoderma. 232-234: 198-207.

Prettyman, G.W. and E.L. McCoy. 2003. Profile layering, root zone permeability, and slope affect on soil water content during putting green drainage. Crop Science. 43: 985-994.

Raturi, S., K.R. Islam, M.J. Carroll, and R.L. Hill. 2005. Thatch and soil characteristics of cool- and warm-season turfgrasses. Communications in Soil Science and Plant Analysis. 35: 2161-2176.

Ren, X., N. Hong, L. Li, J. Kang, and J. Li. 2020. Effect of infiltration rate changes in urban soils on stormwater runoff process. Geoderma. 363: 114158.

Ritsema, C.J., J.C. van Dam, L.W. Dekker, and K. Oostindie. 2001. Principles and modeling of flow and transport in water repellant surface layers, and consequences for management. International Turfgrass Society Research Journal. 9: 615-623.

Ritsema, C.J., L.W. Dekker, J.C. van Dann, and K. Oostindie. 2004. Principles of flow and transport in turfgrass profiles, and consequences for management. Acta Horticulturae. 661: 137-144.

Rowland, J.H., J.L. Cisar, G.H. Snyder, J.B. Sartain, and A.L. Wright. 2009. USGA ultradwarf bermudagrass putting green properties as affected by cultural practices. Agronomy Journal. 101: 1565-1572.

Sammartino, S., E. Michel, and Y. Capowiez. 2012. A novel method to visualize and characterize preferential flow in undisturbed soil cores by using multslice helical CT. Vadose Zone Journal. doi:10.2136/vzj2011.0100.

Schneider, A., F. Hirsch, A. Raab, and T. Raab. 2018. Dye tracer visualization of infiltration patterns in soils on relict charcoal hearths. Frontiers in Environmental Science. 6: 143.

Schmid, C.J., R.E. Gaussoin, R.C. Shearman, M. Mamo, and C.S. Wortmann. 2014. Cultivation effects on organic matter concentration and infiltration rates of two creeping bentgass (Agrostis Stolonifera L.) putting greens. Applied Turfgrass Science. doi10.2134/ATS-2014-0032-RS.

Shein, E.V., D.I. Shcheglov, A.B. Umarova, I.V. Sokolova, and E.Y. Milanovskii. 2009. Structural status of technogenic soils and the development of preferential water flows. Eurasian Soil Science. 42: 636-644.

Skaalsveen, K., J. Ingram, and L.E. Clarke. 2019. The effect of no-till farming on the soil functions of water purification and retention in north-western Europe: A literature review. Soil and Tillage Research. 189: 98-109.

Song, E., J.G. Schneider, S.H. Anderson, K.W. Goyne, and X. Xiong. 2014. Wetting agent influence on water infiltration into hydrophobic sand: II. Physical properties. Agronomy Journal. 106: 1879-1885.

Sorokovsky, P., M. Krzic, and M.D. Novak. 2006. Core aeration of sand-based putting greens in the lower Fraser valley of British Columbia. Canadian Journal of Soil Science. 87: 103-111.

Stock, O. and N.K. Downes. 2008. Effects of additions of organic matter on the penetration resistance of glacial till for the entire water tension range. Soil and Tillage Research. 99: 191-201.

Stumpp, C., W. Stichler, M. Kandolf, and J. Simunek. 2012. Effects of land coer and fertilization method on water flow and solute transport in five lysimeters: A long-term study using stable water isotopes. Vadose Zone Journal. doi:10.2136/vzj2011.0075 .

Tekeste, M.Z., R.L. Raper, and E.B. Schwab. 2008. Soil drying effects on soil strength and depth of hardpan layers as determined from cone index data. Agricultural Engineering International: the CIGR Ejournal. Manuscript LW 07 010.

Tonguc, F. and H. Merdun. 2009. Solute movement in an intact soil core under different ponding heights. Eurasian Soil Science. 42: 1497-1503.

USGA. 2002. Building the USGA green: Tips for success. United States Golf Association.

USGA. 2018. USGA recommendations for a method of putting green construction. United States Golf Association.

Waltz Jr., F.C., V.L. Quisenberry, and L.B. McCarty. 2003. Physical and hydraulic properties of rootzone mixes amended with inorganics for golf putting greens. Agronomy Journal. 95: 395-404.

Wang, K., R. Zhang, and H. Yasuda. 2006. Characterizing heterogeneity of soil water flow by dye infiltration experiments. Journal of Hydrology. 328: 559-571.

Wightman, S. 1994. Making sense out of modified rootzones. Sports Turf. p. 16-19

Woltemade, C.J. 2010. Impact of residential soil disturbance on infiltration rate and stormwater runoff. Journal of the American Water Resources Assoiciation. 46: 700-711.

Woodham, P. 2013. The curse of the black death: Recognizing and managing black layer symptoms in golf greens and sports fields. Bulletin. 261: 34-36.

Yuan, W., N.K. Wijewardane, and S. Jenkins. 2019. Early prediction of soybean traits through color and texture features of canopy RGB imagery. Science Report. 9,14089. https://doi.org/10.1038/s41598-019-50480-x.

Zhang, Y., M. Zhang, J. Niu, and H. Zheng. 2016. The preferential flow of soil: A widespread phenomenon in pedological perspectives. Eurasian Soil Science. 49: 661-672.

Zhang, J., T. Lei, L. Qu, P. Chen, X. Gao, C. Chen, L. Yuan, M. Zhang, and G. Su. 2017. Method to measure soil matrix infiltration in forest soil. Journal of Hydrology. 552: 241-248.

Zhang, Y., Z. Cao, F. Hou, and J. Cheng. 2021. Characterizing preferential flow paths in texturally similar soils under different land uses by combining drainage and dye-staining methods. Water. 13(219). doi.org/10.3390/w13020219.

Zhou, L. and H.M. Selim. 2001. Solute transport in layered soils: Nonlinear and kinetic reactivity. Soil Science Society of America Journal. 65: 1056-1064.